JOURNAL OF MATERIALS SCIENCE 26 (1991) 1851–1855

Reversible short-range ordering due to the structural relaxation in amorphous Ni–Cr–B alloys

O. HARUYAMA, N. ASAHI
Science University of Tokyo, Faculty of Science and Technology, Department of Physics, Noda, Chiba, 278 Japan

Reversible short-range ordering due to the structural relaxation in two amorphous alloys, $Ni_{68}Cr_{14}B_{18}$ (Allied Chemical MBF-80) and melt-spun $Ni_{55}Cr_{25}B_{20}$, was investigated. Excess endothermic peaks were observed in differential scanning calorimetry (DSC) thermograms taken for $Ni_{68}Cr_{14}B_{18}$ alloy annealed for both 5 and 20 h at 493 K, and this phenomenon can be explained as the decomposition process of short range order formed during annealing. Reversible changes in electrical resistance with isochronal annealing temperature were found in both alloys, which may be caused by the reversible formation and the decomposition processes of short range order. Kinetics of reversible relaxation in $Ni_{55}Cr_{25}B_{20}$ alloy was also examined under the assumption that the relaxation process exhibits a Gaussian distribution in the logarithm of the relaxation time, that is, a log normal distribution. The mean relaxation time τ_m is obtained as an Arrhenius type, $\tau_m = \nu_0^{-1} \exp(E_m/k_B T_a)$, where k_B and T_a are Boltzmann constant and annealing temperature, respectively. As the mean activation energy, E_m, and the attempt frequency ν_0, values of 2.20 eV and 1.6×10^{16} sec^{-1} were obtained.

1. Introduction

It is well known that an amorphous alloy changes its properties within the amorphous state by annealing well below crystallization temperature. This phenomenon is called the structural relaxation [1] and generally attributed to atomic rearrangements within the amorphous state [2, 3]. The structure relaxation strongly depends on thermal history of the sample. The reversible structural relaxation, which is often called the chemical short range ordering (CSRO), was observed around 150 K lower than the glass transition temperature, T_g. Furthermore, the annihilation of quenched-in free volume (density fluctuation in a sample), which is called the topological short range ordering (TSRO) and is the irreversible change within the amorphous phase, became extensive in the same temperature region. However, TSRO change can be suppressed by adequate heat treatment at a temperature above the region which CSRO takes place [2, 4, 21].

The reversible structural relaxation was observed in many metal–metal and metal–metalloid amorphous alloys through the reversible changes of physical properties such as Curie temperature [5, 6, 22], elastic modulus [3, 7], specific heat [8] and electrical resistivity [2, 4, 9]. The reversible relaxation process was generally proposed to originate in compositional atomic rearrangements in short range. Balanzat *et al.* [2] explained the reversible change in electrical resistance as the short range ordering analogous to it observed in crystalline alloys. Another model was also proposed by O'Handley and co-workers [10, 11] that the reversible relaxation process can be attributed to the transition of a basic unit in the amorphous structure between a tetragonal unit and an octahedral one. Inoue *et al.* [12] have systematically investigated the effect of composition on the anneal-induced enthalpy relaxation and observed an excess endothermic reaction upon heating the sample annealed at a temperature well below T_g. They considered this phenomenon as local and medium range atomic rearrangements upon annealing.

Kinetics of short range ordering due to the reversible relaxation has been studied by many workers, and some models have been proposed to explain the mechanism. Van den Buekel *et al.* [7] pointed out that it is necessary to treat reversible structural relaxation processes as distributed continuously in activation energy (AES model), in order to account for the wide range of annealing temperatures and times over which reversible relaxation effects are seen. Gibbs and co-workers [13, 14] described the relaxation processes at first as the transition between the levels of a single two-level system (TLS model) with the activation energy spectrum and later went on to use a relatively large amount of two-level systems with small energy splittings to account for large reversible structure changes.

In Ni–TM (TM: transition metal) based amorphous alloys, the cases of TM=Fe [4, 8], CO [12], Ti [2], Zr [15, 16] and Pd [17] have exhibited the reversible relaxation, but the criterion to identify which combination of metallic elements cause the reversible relaxa-

0022–2461/91 $03.00 + .12

tion is not yet discovered. So it is important to check which alloy systems generate the reversible relaxation and to investigate its mechanism. The purpose of this study is to show that the reversible relaxation was observed in Ni–Cr based amorphous alloy and also to examine the kinetics of reversible relaxation.

2. Experimental procedure

An amorphous $Ni_{68}Cr_{14}B_{18}$ alloy was obtained from Allied Chemical Co. Ltd, about 25 mm in width and 40 μm in thickness. Ribbons, about 2 mm in width and 20 μm in thickness, with the composition of $Ni_{55}Cr_{25}B_{20}$ were produced by a melt spinning apparatus operated in a reduced Ar atmosphere with a cupper roller of 10 cm in radius. X-ray diffraction scans with Co$K\alpha$ radiation did not show any sign of crystallinity in the samples. Heat treatments of samples were performed with an infrared furnace in a He atmosphere. The samples were heated at a rate of 300 K min^{-1} to given annealing temperatures T_a, at which they were annealed isothermally. After isochronal and isothermal anneals, samples were quickly cooled to room temperature and then electrical resistances were measured at 78 K with a d.c. four-probe method, where the accuracy of resistance were controlled within ± 0.004%. To decide the crystallization temperature T_x of samples, electrical resistance curves and DSC thermograms were taken with a heating rate of 20 K min^{-1}. T_x obtained by both methods were almost coincident with each other. The changes in specific heat of samples were calculated from the DSC thermograms, using a Rigaku DSC model 8240, where an aluminium chip in 99.99 at % purity was used as a standard material.

3. Results and discussion

3.1. Crystallization temperature and pre-annealing condition

As mentioned, the adequate heat treatment at T_p (pre-annealing temperature) enables one to induce the reversible relaxation during annealing below T_p, because the annihilation of quenched-in free volume becomes negligible owing to the stabilization of amorphous structure by pre-annealing. To find out the appropriate pre-annealing condition, the change of amorphous properties around T_x must be examined. Fig. 1 shows electrical resistance curve as a function of temperature and DSC thermograms taken with a heating rate of 20 K min^{-1}. From Fig. 1, T_x were determined as 664 K in $Ni_{68}Cr_{14}B_{18}$ alloy and 710 K in $Ni_{55}Cr_{25}B_{20}$ alloy, respectively. Reduced resistance ratios $\Delta R/R_{as}$ in as-quenched samples are shown in Fig. 2 as a function of isochronal annealing temperature, where R_{as} represents the value of electrical resistance measured in an as-quenched condition and ΔR is defined as $R(T_a) - R_{as}$. Both curves initially increase with rising annealing temperature. Beyond the peak temperature, about 540 K in both alloys, they begin to decrease. These behaviours are similar to ones observed in a lot of alloys [4, 9, 18] and are explained as below. In the low temperature region (below the peak temperature), short range ordering

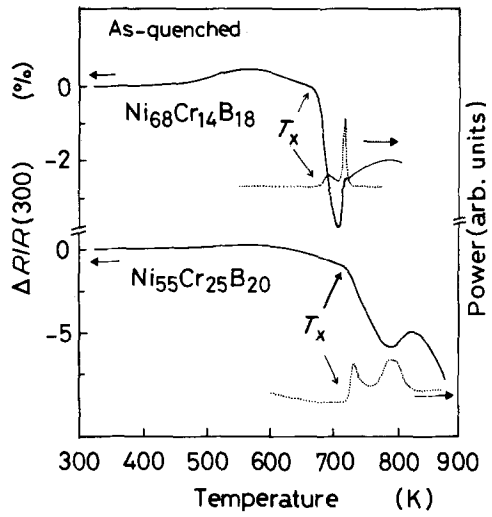

Figure 1 Electrical resistance change (solid line) and DSC curve (dotted line) observed on heating at a rate of 20 K min^{-1} for $Ni_{68}Cr_{14}B_{18}$ and $Ni_{55}Cr_{25}B_{20}$ alloys.

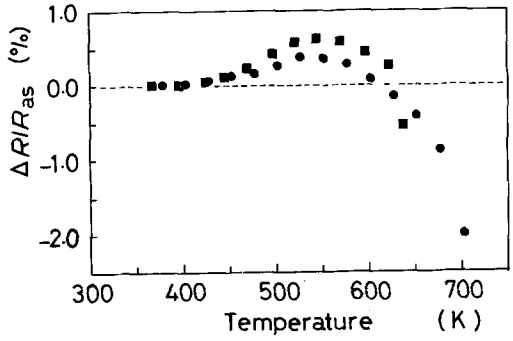

Figure 2 Resistance changes $\Delta R/R_{as}$ of as-quenched (■) $Ni_{68}Cr_{14}B_{18}$ and (●) $Ni_{55}Cr_{25}B_{20}$ alloys during isochronal annealing for 10 min.

TABLE I Crystallization temperature T_x and pre-annealing temperature T_p for $Ni_{68}Cr_{14}B_{18}$ and $Ni_{55}Cr_{25}B_{20}$ alloys

Amorphous	T_x (K)	T_p (K)
$Ni_{68}Cr_{14}B_{18}$	664	623
$Ni_{55}Cr_{25}B_{20}$	710	638

may progress during isochronal annealing together with decay of the chemical disorder state, which was frozen in samples by quenching from the melt. In the high temperature region, the order state formed during annealing may be decomposed to the disorder state, which is more thermodynamically stable in the high temperature region, and simultaneously the annihilation of quenched-in free volume takes place. T_p was determined on the basis of the above explanations and is listed in Table I together with T_x for each sample.

3.2. Thermally-induced short range order

3.2.1. Change in specific heat

Thermal scans by DSC were carried out to examine the changes in specific heat for as-quenched and annealed $Ni_{68}Cr_{14}B_{18}$ alloys. The temperature dependence of specific heat is shown in Fig. 3. Curves 1 and 2

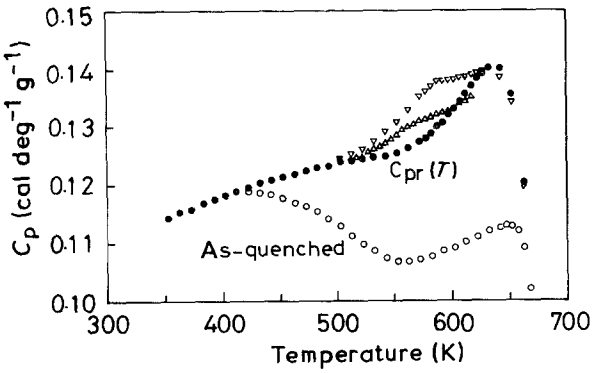

Figure 3 Temperature dependence of specific heat for as-quenched and annealed at 493 K for (Δ) 5 h, (V)20 h, $Ni_{68}Cr_{14}B_{18}$ alloy which was pre-annealed at 622 K for 5 min. The specific heat was calçulated from DSC thermogram taken with a heating rate of 20 K min^{-1}.

indicate the changes in specific heat of the samples which were annealed at 493 K for 5 and 20 h, respectively, then stabilized by a 5 min pre-anneal at 622 K. The reference curve $C_{pr}(T)$ was obtained from a DSC thermogram taken subsequent to pre-annealing. The specific heat of the annealed sample shows a behaviour which follows a $C_{pr}(T)$ up to about 490 K, and hereafter exhibits an excess specific heat relative to the reference curve. The occurrence of the excess specific heat is interpreted as the decomposition process of short range order thermally induced during long time annealing at 493 K.

3.2.2. Reversible resistance change

The resistance measurements were carried out during isochronal up- and down-anneals subsequent to pre-annealing to check whether the reversible relaxation appears or not. Fig. 4 shows the changes in reduced resistance ratio with isochronal annealing temperature, where R_p represents the value of resistance measured immediately after pre-annealing for 10 min in $Ni_{68}Cr_{14}B_{18}$ and for 45 min in $Ni_{55}Cr_{25}B_{20}$ alloys, respectively. The first and third run were taken with down-anneals and the second run was measured with up-anneals. For $Ni_{55}Cr_{25}B_{20}$ alloy, the third run has a similar behaviour to the first one, and the reversible change in resistance is clearly observed. This suggests that the pre-annealing stabilized the amorphous structure and the resistance change due to the free volume change did not occur during up- and down-anneal cycles. On the other hand, the third run for $Ni_{68}Cr_{14}B_{18}$ alloy shifts to a lower position than the first run, and this means the irreversible part in relaxation process still existed together with reversible one due to insufficient pre-annealing temperature. $\Delta R/R_p$ for $Ni_{55}Cr_{25}B_{20}$ alloys remains unchanged until about $T_s = 550$ K and beyond T_s it decreases almost linearly. This behaviour is explained as mentioned below. At each annealing temperature above T_s, the thermal equilibrium state of short range ordering is attained during the time duration of a heat treatment owing to the high mobility of atoms but below T_s, in contrast to this, the equilibrium order state is not achieved due to lack of thermal energy. Then, al-

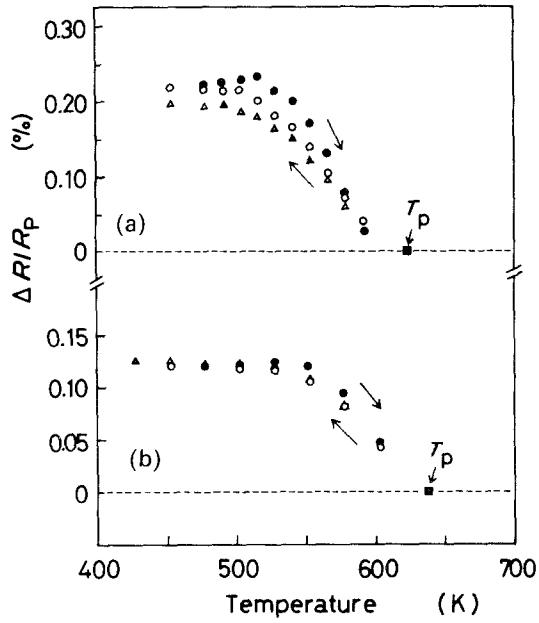

Figure 4 Resistance changes $\Delta R/R_p$ of pre-annealed samples during isochronal up- and down-anneal cycles; (a) $Ni_{68}Cr_{14}B_{18}$ alloy: pre-annealed at 623 K for 10 min; (b) $Ni_{55}Cr_{25}B_{20}$ alloy: pre-annealed at 638 K for 45 min; (○) first run, (●) second run, (△) third run.

though $\Delta R/R_p$ remains apparently unchanged, a longer annealing may approach the formation of equilibrium short range order. The change in $\Delta R/R_p$ between about 550 and 600 K, where the linear relation between $\Delta R/R_p$ and annealing temperature was seen, is about -1.4×10^{-5} K^{-1} for $Ni_{55}Cr_{25}B_{20}$ alloy. This value is comparable to -1.2×10^{-5} K^{-1} for $Ni_{40}Fe_{40}P_{14}B_6$ alloy [18].

3.3. Kinetics of short range ordering

To examine the kinetics of short range ordering, isothermal changes in resistance were measured for $Ni_{55}Cr_{25}B_{20}$ alloy. As shown in Fig. 2, this alloy has a higher T_p than that in $Ni_{68}Cr_{14}B_{18}$ alloy. Therefore, the formation of short range order during pre-annealing would be suppressed to a lower level. Fig. 5 shows the changes in $\Delta R/R_p$ during typical isothermal anneals at $T_a = 563$ and 593 K. During an early stage of annealing, the value of $\Delta R/R_p$ on annealing at 563 K is smaller than that obtained at 593 K, but it's equilibrium value $(\Delta R/R_p)_{eq}$ is larger on annealing at 563 K. Fig. 6 shows the T_a dependence of $(\Delta R/R_p)_{1\ min}$, the value of $\Delta R/R_p$ at $t_a = 1$ min, and $(\Delta R/R_p)_{eq}$. $(\Delta R/R_p)_{1\ min}$ increases with T_a and $(\Delta R/R_p)_{eq}$ decreases with T_a. The different values of $(\Delta R/R_p)_{eq}$ in Fig. 6 suggest a relaxation process with a distribution of relaxation time [19]. The $\Delta R/R_p$ normalized by $(\Delta R/R_p)_{eq}$ is shown in Fig. 7. In this case, the curves do not cross mutually. It has been reported in many alloys [6, 9, 20] that the kinetics of reversible relaxation was well described by the process with a Gaussian distribution in the logarithm of relaxation time (a log normal distribution). Since the relaxation process may be expected to be controlled by atom movements, we assume here that the relaxation time has an Arrhenius form as $\tau = \nu_0^{-1} \exp(E/k_B T_a)$, where ν_0, E and k_B are the attempt frequency, the activation energy and

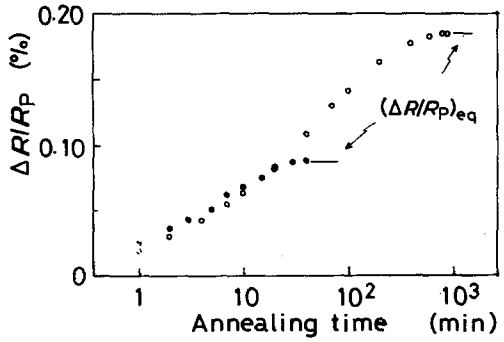

Figure 5 Resistance changes $\Delta R/R_p$ of pre-annealed at 638 K for 45 min, $Ni_{55}Cr_{25}B_{20}$ alloy during isothermal anneals at (○) 563 and (●) 593 K.

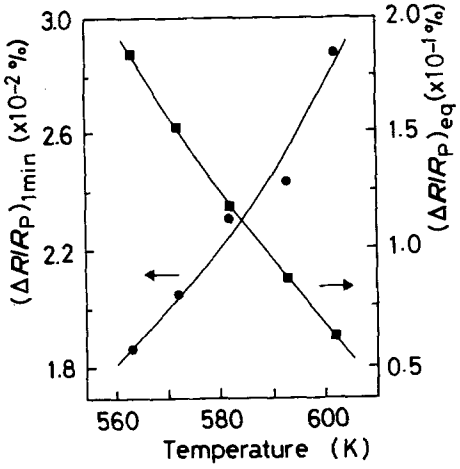

Figure 6 Values of $\Delta R/R_p$ in pre-annealed at 638 K for 45 min, $Ni_{55}Cr_{25}B_{20}$ alloy after a 1 min anneal, $(\Delta R/R_p)_{1\,min}$, and in an equilibrium order state, $(\Delta R/R_p)_{eq}$, for various isothermal annealing temperatures.

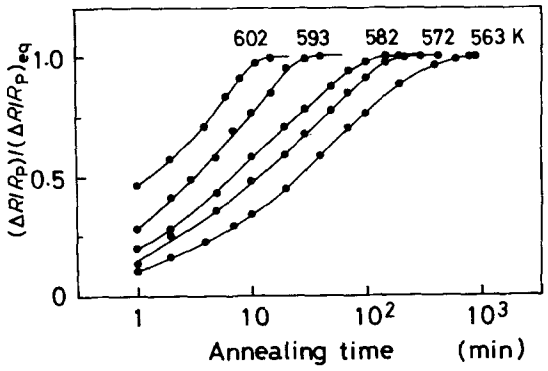

Figure 7 Normalized resistance changes $\Delta R/R_p/(\Delta R/R_p)_{eq}$ for pre-annealed at 638 K for 45 min, $Ni_{55}Cr_{25}B_{20}$ alloy during isothermal annealing.

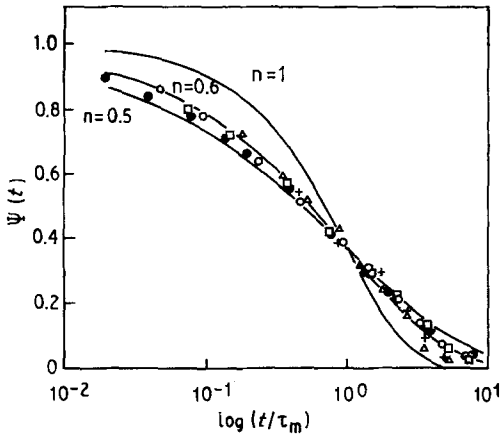

Figure 8 Relaxation function $\psi(t) = 1 - \Delta R/R_p/(\Delta R/R_p)_{eq}$ for pre-annealed $Ni_{55}Cr_{25}B_{20}$ alloy as a function of $\log(t/\tau_m)$. Theoretical curves for $n = 0.5$, 0.6 and 1 are drawn in solid lines; (●) 563, (○) 572, (□) 583, (△) 593, (+) 603 K.

Boltzmann constant, respectively. Then it is assumed that the attempt frequency has a constant value and the value of activitation energy has a Gaussian distribution. The relaxation function $\psi(t)$ is related to the physical property $P(t)$ by assuming first order kinetics of a process with the relaxation time τ as below [5],

$$\psi(t) = \frac{P(t) - P_\infty}{P_0 - P_\infty} = \int_0^\infty G(\tau)\exp(-t/\tau)d\tau \quad (1)$$

where P_0 and P_∞ are an initial and equilibrium values of $P(t)$. The distribution function $G(\tau)$ is normalized such that

$$\int_0^\infty G(\tau)d\tau = 1 \quad (2)$$

Equation 1 is conventionally approximated to the next expression,

$$\psi(t) \approx \exp\{-(t/\tau_m)^n\} \quad (3)$$

where τ_m is the mean relaxation time and the inverse of an exponent n, which represents the width of distribution of relaxation time. Thus, the mean relaxation time τ_m is represented as $\tau_m = \nu_0^{-1}\exp(E_m/k_B T_a)$, where E_m is the mean activation energy. Substituting $P(t) = \Delta R/R_p$, $P_0 = 0$ and $P_\infty = (\Delta R/R_p)_{eq}$ into Equation 1, the relaxation functions for various annealing temperature are fitted to Equation 3 by using the least square method. Then the parameters n and τ_m were obtained for each annealing temperature. The relaxation functions obtained are plotted as a function of $\log(t/\tau_m)$ in Fig. 8. The data are well described by Equation 3 with the mean value of $n \approx 0.60$. In order

TABLE II Kinetic parameters for short range ordering in amorphous $Ni_{55}Cr_{25}B_{20}$ alloy together with other alloys

Amorphous	n	E_m (eV)	ν_0^{-1} (sec^{-1})	Method	Reference
$Ni_{40}Fe_{40}P_{14}B_6$	0.5	1.39	1.8×10^{12}	electrical resistance	[18]
$Ni_{40}Fe_{40}B_{20}$	0.4	1.75	–	Young's modulus	[3]
$Ni_{63}Fe_{15}Si_8B_{14}$	0.43	1.93	1.2×10^{15}	electrical resistivity	[4]
$(Co_{1-x}Fe_x)_{75}Si_{10}B_{15}$ $x = 0.067, 0.1, 0.25, 0.5$	0.37 ~ 0.43	1.78 ~ 2.70	$5.3 \times 10^{12} \sim 2.4 \times 10^{20}$	electrical resistivity	[9]
$Ni_{55}Cr_{25}B_{20}$	0.60	2.20	1.6×10^{16}	electrical resistance	This work

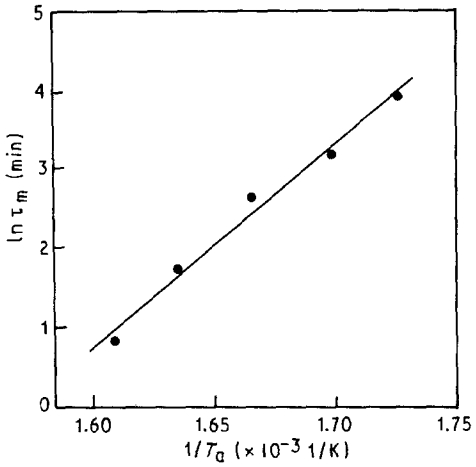

Figure 9 Relation between $\ln\tau_m$ and T_a^{-1} for pre-annealed $Ni_{55}Cr_{25}B_{20}$ alloy.

to estimate the parameters ν_0 and E_m, the plot between $\ln\tau_m$ and T_a^{-1} is shown in Fig. 9. The values of the kinetic parameters obtained are summarized in Table II together with those found in other alloys. The values of $\nu_0 = 1.6 \times 10^{16}$ sec^{-1} and $E_m = 2.20$ eV obtained from this experiment are reasonable in comparison with those reported in other alloys. On the other hand, the mean value of exponent n is slightly larger. This means that $Ni_{55}Cr_{25}B_{20}$ alloy has a slightly narrower width of the distribution of relaxation time. This fact would suggest that the fluctuation of the amorphous structure was partly diminished by the prestabilization due to the longer pre-annealing, and consequently the degree of freedom in atom displacements was decreased. Komatsu and Matusita [4] have suggested that in $Ni_{63}Fe_{15}Si_8B_{14}$ amorphous alloy reversible short range ordering could be well described by movements of nickel and iron atom in a trigonal prism which is considered as a basic unit in $TM_{75}M_{25}$ (TM: transition metal, M: metalloid) amorphous alloy. O'Handley [10] has proposed the structural model that reversible short range ordering corresponds to the mutual transition of a basic unit in amorphous structure between a tetragonal and octahedral unit during annealing. However, it is hard to find out from this experiment the structural model applicable to the reversible relaxation mechanism in Ni–Cr–B amorphous alloy. More extensive study for short range ordering in Ni–TM based alloys is in progress.

4. Conclusion

The reversible structural relaxation was confirmed in two Ni–Cr–B based amorphous alloy, $Ni_{68}Cr_{14}B_{18}$ and $Ni_{55}Cr_{25}B_{20}$, by an excess endothermic reaction observed in DSC thermograms and reversible changes in electrical resistance with isochronal annealing. Using $Ni_{55}Cr_{25}B_{20}$ alloy with higher pre-annealing temperature, kinetics of reversible relaxation was examined through isothermal measurements of electrical resistance. Under the activation energy spectrum model, the kinetic parameters were determined to be about 0.60 for n, 2.20 eV for activation energy and 1.6×10^{16} sec^{-1} for the attempt frequency.

References

1. T. EGAMI, *Mater. Res. Bull.* **13** (1978) 557.
2. E. BALANZAT, J. T. STANLEY, C. MAIRY and J. HILLAIRET, *Acta Metall.* **33** (1985) 785.
3. M. G. SCOTT and A. KURSUMOVIC, *ibid.* **30** (1982) 853.
4. T. KOMATSU and K. MATUSITA, *J. Mater. Sci.* **21** (1986) 1693.
5. A. L. GREER, M. R. J. GIBBS, J. A. LEAKE and J. E. EVETTS, *J. Non-Cryst. Solids* **38, 39** (1980) 379.
6. M. BOURROUS and F. VARRET, *Solid State Commun.* **57** (1986) 713.
7. A. VAN DEN BEUKEL, S. VAN DER ZWAAG and A. L. MULDER, *Acta Metall.* **32** (1984) 1895.
8. R. BRÜNING, Z. ALTOUNIAN and J. O. STRÖMOLSEN, *J. Appl. Phys.* **62** (1987) 3633.
9. T. KOMATSU, K. IWASAKI, S. SATO and K. MATSUSITA, *ibid.* **64** (1988) 4853.
10. R. C. O'HANDLEY, B. W. CORB, J. MEGUSAR and N. J. GRANT, *J. Non-Cryst. Solids* **61, 62** (1984) 773.
11. J. M. RIVEIRO, V. MADURGA and A. HERNANDO, *Phys. Rev. B* **39** (1989) 11950.
12. A. INOUE, T. MASUMOTO and H. S. CHEN, *J. Mater. Sci.* **19** (1984) 3953.
13. M. R. J. GIBBS, J. E. EVETTS and J. A. LEAKE, *ibid.* **18** (1983) 278.
14. G. HYGATE and M. R. J. GIBBS, *J. Phys. F Met. Phys.* **17** (1987) 815.
15. J. HILLAIRET, E. BALANZAT, N. E. DERRADJI and A. CHAMBEROD, *J. Non-Cryst. Solids* **61, 62** (1984) 781.
16. S. LEFEBVRE, M. HARMELIN, A. QUIVY, J. BIGOT and Y. CALVAYRAC, *Z. Phys.* **157** (1988) 365.
17. J. D. COMINS, J. E. MACRONALD, M. R. J. GIBBS and G. A. SAUNDERS, *J. Phys. F Met. Phys.* **17** (1987) 19.
18. Y. TAKAHARA, K. HATADE and H. MATSUDA, *Mater. Trans. JIM* **29** (1988) 774.
19. A. S. NOWICK and B. S. BERRY, *IBM. J. Rev. Dev.* **5** (1961) 297.
20. J. A. LEAKE, *Key Eng. Mater.* **13–15** (1987) 151.
21. A. VAN DEN BEUKEL, *J. Non-Cryst. Solids* **83** (1986) 134.
22. H. Q. GUO, W. FERNENGEL, A. HOFMANN and H. KRONMULLER, *IEEE Trans. Mag.* MAG-20 (1984) 1394.

Received 2 January
and accepted 16 May 1990